

# One pot three component synthesis of substituted 3,4,6,7-tetrahydro-3,3,6,6-tetramethyl-9,10-diphenylacridine-1,8(2H,5H,9H,10H)-diones catalyzed by efficient $\text{In}_2\text{O}_3\text{-SiO}_2$

Deepak Totaram Tayde (✉ [dtc\\_chem@yahoo.com](mailto:dtc_chem@yahoo.com))

MJM ACS College karanjali <https://orcid.org/0000-0001-9187-4261>

Madhukar E. Navgire

Jijamata ACS College, Bhenda

Machhindra K. Lande

Dr Babasaheb Ambedkar Marathwada University

---

## Research Article

**Keywords:**  $\text{In}_2\text{O}_3\text{-SiO}_2$ , Hydrothermal method, Heterocyclic compound, Acridine

**Posted Date:** September 21st, 2021

**DOI:** <https://doi.org/10.21203/rs.3.rs-899408/v1>

**License:**   This work is licensed under a Creative Commons Attribution 4.0 International License.

[Read Full License](#)

---

**Version of Record:** A version of this preprint was published at Polycyclic Aromatic Compounds on November 23rd, 2021. See the published version at <https://doi.org/10.1080/10406638.2021.2006249>.

# Abstract

A convenient, One pot synthesis of heterocyclic nucleous acridine derivative compound has been achieved those are having very much attention in medicinal chemistry because of their extensive application in biology. The mixture of dimedone, substituted benzaldehyde and aniline were catalyzed by efficient  $\text{In}_2\text{O}_3\text{-SiO}_2$  heterogeneous reusable catalyst in ethanol to obtain the desired acridine derivatives with good yield. Hydrothermal method used to synthesize  $\text{In}_2\text{O}_3\text{-SiO}_2$  catalytic material. This catalytic material were characterized by using X-ray diffraction spectroscopy (XRD), scanning electron microscopy (SEM), Energy dispersive spectroscopy (EDS), Fourier transform infrared spectroscopy (FT-IR), Transmission electron microscope (TEM), Temperature-programmed desorption ( $\text{NH}_3$ -TPD) and Brunauer-Emmett-Teller (BET). Our synthetic strategy features high yield, simple work up procedure, non-toxic, clean, and easy recovery and reusability of the catalytic system.

## 1. Introduction

The discovery of a new nitrogen containing basic material in the anthracene fraction of coal tar was announced by Graebe and Carol in 1870. The difference between anthracene and acridine is one of the CH group is replaced by nitrogen. Due to its acrid smell and irritating action on the skin and mucous membrane, this new substance was called "acridin" (acris = sharp, or pungent) [1]. In 1912, Ehrlich and Benda first proposed that acridine has been used an antimicrobial agent and its clinical used occurred in 1917. [2] The synthesis of acridine and analogues has attracted considerable attention from organic and medicinal chemists for many years, as a number of natural sources have been reported to have this heterocyclic nucleus [3–6]. Acridines moiety has been utilized in the electronic devices, electroluminescence devices and light-emitting diodes for this there is a file european patent by Fadhel and Pretsch [7]. 1,8-Dioxodecahydroacridines and their derivatives are poly-functionalized [8, 9]. Acridine derivatives have been used to synthesize labeled conjugates with medicinals, peptides, proteins and nucleic acids that exhibit antitumor and DNA-binding properties [10–16]. Many members of this family are nowadays used for the treatment of platelet anti aggregatory activity, Alzheimer's disease, tumors, cardiovascular diseases including hypertension and diabetes [17–22]. They are found to be potent drugs towards metastatic breast cancer cell. Acridine have been utilized as single agents or in combination with other antineoplastic drug in treatment of acute non-lymphocytic and lymphocytic leukemia and against lung cancer. Acridine inhibit RNA synthesis.

Literature survey, the 1,8- dioxo-decahydroacridines synthesised by various researchers have been reported, in which 1,3-Di (bromo or chloro)-5,5-Dimethylhydantoin [23], Sulfonic acid functionlized silica ( $\text{SiO}_2\text{-Pr-SO}_3\text{H}$ ) [24], nano- $\text{Fe}_2\text{O}_3$  [25], HCl [26],  $\text{Fe}_3\text{O}_4\text{@SiO}_2\text{-MoO}_3\text{H}$  nanoparticles [27], Ru-catalyst [28], Ionic liquid with multi- $\text{SO}_3\text{H}$  groups [29] like this various catalyst were used for the synthesis but  $\text{In}_2\text{O}_3\text{-SiO}_2$  combination of binary mixed metal oxide till this date not utilized for it.

In this 20th century, the world is very fast and everyone doesn't have enough time. There is need to develop an expedient heterogeneous catalyst which is having the capacity to do multi component

reaction in one step with reducing the rate of chemical reaction. In continuation of our studies about to prepared multifunctional mixed metal oxides and utilized in organic transformation [30–33]. Here,  $\text{In}_2\text{O}_3$  is basically considered as basic solid, but when it's doped with another metals its acidity decreases and basicity increases [34]. Literature survey, there were prepare the new design of novel catalytic material,  $\text{In}_2\text{O}_3$  is doped with different type metals to synthesized a ternary mixture of metal oxides and utilize for various transformations and gas sensing properties [35] but binary mixture of  $\text{In}_2\text{O}_3$ - $\text{SiO}_2$  as solid heterogeneous catalyst in organic transformation reaction is not studied well till this date. However, crystalline  $\text{In}_2\text{O}_3$  combine with mesoporous  $\text{SiO}_2$  by hydrothermal method to form the multifunctional, cost effective, nontoxic and eco-friendly catalyst. Thus, it is convenient for us, to have less effort because of simple experimental method for separation and environmentally benign catalyst.

To shed light on the catalytic activity of  $\text{In}_2\text{O}_3$ - $\text{SiO}_2$  of solid heterogeneous catalyst has been tested. Here we report, a  $\text{In}_2\text{O}_3$ - $\text{SiO}_2$  catalyst utilized for the synthesis of substituted 3,4,6,7-tetrahydro-3,3,6,6-tetramethyl-9,10-diphenylacridine-1,8(2H,5H,9H,10H)-diones derivatives using multicomponent reaction between dimedone, substituted benzaldehyde and aniline under reflux condition with ethanol as solvent. The developed protocol has several benefits such as short reaction time, mild reaction condition, reusability of catalyst.

Nowadays, research in organic transformations with solvent have drawn great interest, particularly from the viewpoint to enhance the rate of reaction because solvent generate the phase which is helpful for reaction mixture molecules interaction with catalyst [36–39].

Moreover, some novel products can be obtained only from liquid phase reactions rather than from the solvent-free reactions especially in the field of chemistry. Liquid phase generate mobile phase which is useful for the molecular interaction in the reaction mixture. Solid state reactions are simple to handle, reduce pollution, comparatively cheap to operate and are especially important in industry [40–42]. So that for synthesis of acridine derivative to use solvent environment.

## 2. Results And Discussion

At first to optimize the reaction condition, we studied the reaction of dimedone (2 mmol), benzaldehyde (1mmol), and aniline (1mmol) as model compound in the presence of  $\text{In}_2\text{O}_3$ - $\text{SiO}_2$  (1g) as catalysts in this reaction. We evaluated the effect of different solvents such as  $\text{CH}_2\text{Cl}_2$ , EtOH,  $\text{H}_2\text{O}$ , MeCN, DMF and solvent-free condition on the reaction rate under the same reaction conditions. EtOH solvent afforded the products in higher yield and shorter reaction time (Table 1).

Table 1  
Optimization of model reaction (4a) using several solvent.

Entry	Solvent	Time (min)	Yield (%) <sup>b</sup>
1	Solvent free	170	-
2	CH <sub>2</sub> Cl <sub>2</sub>	200	43
3	H <sub>2</sub> O	230	30
4	MeCN	190	75
5	DMF	240	70
6	EtOH	100	92

Reaction Condition: dimedone (2 mmol), benzaldehyde (1 mmol) and aniline (1mmol) in In<sub>2</sub>O<sub>3</sub>-SiO<sub>2</sub> catalyst (1 g) EtOH as catalyst; <sup>b</sup>Isolated yields.

In this study the effect of different catalyst are investigated and shown in (**Table 2**). When In<sub>2</sub>O<sub>3</sub> and SiO<sub>2</sub> powder was employed, the corresponding product yield was obtained 60% and 55% respectively (**Table 2, entry 1, 2**). However the model reaction was carried out in In<sub>2</sub>O<sub>3</sub>-SiO<sub>2</sub> which gave 92% yield. We have found that In<sub>2</sub>O<sub>3</sub>-SiO<sub>2</sub> as a better catalyst with respective to reaction time and yield of obtained products.

Table 2  
Synthesis of (4a) using different catalysts.

Entry	Catalyst	Time (min)	Yield (%) <sup>b</sup>
1	In <sub>2</sub> O <sub>3</sub>	160	60
2	SiO <sub>2</sub>	190	55
3	In <sub>2</sub> O <sub>3</sub> -SiO <sub>2</sub>	100	92

Reaction Condition: dimedone (2 mmol), benzaldehyde (1 mmol) and aniline (1mmol) using In<sub>2</sub>O<sub>3</sub>-SiO<sub>2</sub> as catalyst; <sup>b</sup>Isolated yields.

We next investigated the amounts of In<sub>2</sub>O<sub>3</sub>-SiO<sub>2</sub> catalyst (0.3, 0.5, 0.8, 1.0g). The optimum yield of the 1, 8 dioxo-decahydro acridine was obtained when 1g of In<sub>2</sub>O<sub>3</sub>-SiO<sub>2</sub> metal oxide was used (**Table 3**). Therefore, in an optimized reaction condition dimedone (2 mmol), benzaldehyde (1 mmol), aniline (1 mmol) were treated with In<sub>2</sub>O<sub>3</sub>-SiO<sub>2</sub> (1g) and reflux at 80°C for mention time in **Table 4**.

Table 3  
Optimization of amount of catalysis for model reaction (4a).

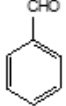
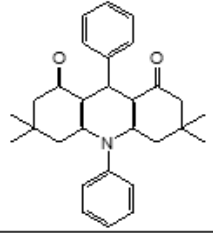
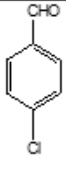
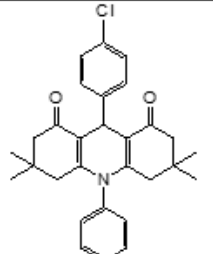
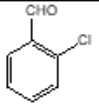
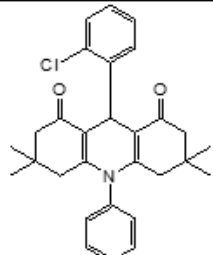
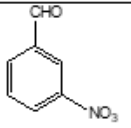
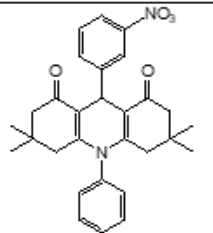
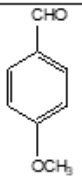
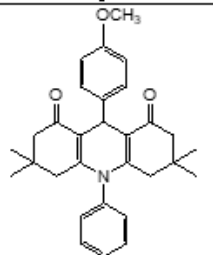
Entry	Catalyst (g)	Yield (%) <sup>b</sup>
1	0.3	54
2	0.5	60
3	0.8	88
4	1.0	92

Reaction Condition: dimedone (2 mmol), benzaldehyde (1 mmol) and aniline (1mmol) using In<sub>2</sub>O<sub>3</sub>-SiO<sub>2</sub> (1g) as catalyst; <sup>b</sup>Isolated yields.

To study the generality of this process, several examples illustrating this method for the synthesis of those polyfunctionalized 1,8-dioxodecahydroacridines were studied. Results are summarized in (Table 4). The effect of substituents on the aromatic ring did show expected strong effects in terms of yields under these reaction conditions. Aromatic aldehyde derivatives containing electron-withdrawing groups (such as nitro and halo groups) or electron-donating groups (such as alkoxyl groups) were employed and they were found to react well to give the corresponding 1,8-dioxodecahydroacridines derivatives in good to excellent yields. Aromatic aldehydes having electron withdrawing groups on the aromatic ring (Table 4, **entries 4b, 4c, 4d**) react faster than electron-donating groups (Table 4, **entry 4e**).

We also examined the recycling performance of In<sub>2</sub>O<sub>3</sub>-SiO<sub>2</sub> catalyst. It was investigated by using the same model reaction. After the separation of product the catalyst was washed with ethanol for two to three times and dried at 95°C and then used directly with fresh substrates under identical conditions without further purification. It was shown that the catalyst could be used for three runs without a noticeable drop in the product yield and its catalytic activity (Fig. 1). The catalyst having easy recycling performance is also an attractive property for the environmental protection and economic reasons.

**Table 4** Synthesis of 1, 8 dioxo-decahydro acridine derivatives.

Entry	Aldehydes	Product	Time (min)	Yield (%) <sup>b</sup>	M.P.(°C)	
					Found	Literature
4a			100	92	210-215	200-205[43]
4b			90	90	240-242	233-235[44]
4c			95	89	235-241	230-234[44]
4d			75	90	278-280	276-278[45]
4e			115	91	285-290	290-291[46]

Reaction condition: Dimedone (2 mmol), Benzaldehyde (1 mmol) and Aniline (1 mmol) in  $\text{In}_2\text{O}_3\text{-SiO}_2$  (1:1) catalyst (1 g) using EtOH as solvent; <sup>b</sup>Isolated yields.

### 3. Experimental

#### 3.1 Synthesis of series of $\text{In}_2\text{O}_3\text{-SiO}_2$ mixed metal oxide by hydrothermal method.

The  $\text{In}_2\text{O}_3\text{-SiO}_2$  mixed metal oxides were prepared by hydrothermal method. It was prepared from the aqueous solution of  $\text{InCl}_3$  and tetraethyl orthosilicate (TEOS) in 5 mL of ethanol to taken in separate beakers respectively. Mixed these two solutions thoroughly in an autoclavable bottle with constant stirring followed by the addition of 1gm cetyl trimethyl ammonium bromide (CTAB) as structural directing

agent. This solution was then hydrolyzed by 10 mL 1:1 aqueous ammonia (aq.  $\text{NH}_3$ ) with constant stirring until the  $\text{pH}$  of solution reached to 9–10. Pale Yellowish precipitate formed, was transferred to the teflon beaker in autoclave. This reaction mixture was heating up to  $150^\circ\text{C}$  with 400 rpm at 58 psi naturally generated pressure with constant stirring of 24 h. After drying at  $110^\circ\text{C}$  for 7 h in an oven, the obtained powder was pulverized using mortar and pestle and finally calcined at  $500^\circ\text{C}$  for 2 h. Similarly, all the pure metal oxides and mixed metal oxides are prepared by following same procedure. Similarly, by using above same procedure there systematic preparations of pure  $\text{SiO}_2$ ,  $\text{In}_2\text{O}_3$  and series of different loading In/Si molar ratio is shows in Table 5.

Table 5  
Synthesis of series of mixed metal oxides by hydrothermal method.

Entry	Mixed metal oxide	Molar ratio
1	$\text{SiO}_2$	1
2	$\text{In}_2\text{O}_3$	1
3	$\text{In}_2\text{O}_3\text{-SiO}_2$	0.8 : 0.2
4	$\text{In}_2\text{O}_3\text{-SiO}_2$	0.2 : 0.8
5	$\text{In}_2\text{O}_3\text{-SiO}_2$	1:1

## 3.2 General procedure for the synthesis of 1,8 dioxo-decahydro acridine 4 (a-e):

The catalytic activity of  $\text{In}_2\text{O}_3\text{-SiO}_2$  catalyst has been tested for synthesis of 1,8 dioxo-decahydro acridine derivatives by using dimedone (2 mmol), substituted benzaldehyde (1 mmol) and aniline (1 mmol) under reflux condition using ethanol (15 mL) as solvent (Scheme 1). Reaction confirmation is checked by TLC analysis. The solvent was removed at under reduced pressure to obtained acridine product in good and excellent yield. The model reaction product characterized by  $^1\text{H}$  NMR, FTIR and Mass spectroscopy. The developed protocol has several benefits such as short reaction time, mild reaction condition, reusability of catalyst.

## 3.3 Spectral Data Of Representative Compound

**3,4,6,7-tetrahydro-3,3,6,6-tetramethyl-9,10-diphenylacridine-1,8(2H,5H,9H,10H)-dione (4a);**

$^1\text{H}$  NMR (300 MHz,  $\text{CDCl}_3$ ):  $\delta$  = 7.17–7.27 (m, 5H, Ar-H), 7.08–7.15 (m, 5H, Ar-H), 5.54 (s, 1H, CH), 2.43 (d, 4H,  $\text{CH}_2$ ), 2.20 (d, 4H,  $\text{CH}_2$ ), 1.09 (s, 6H, 2X  $\text{CH}_3$ ), 0.87 (s, 6H, 2X  $\text{CH}_3$ ); IR (KBr): 2962(C-H stretch), 1589(C=O), 1450(C=C), 1373(C-N),  $m/z$  426.22 ( $\text{M}^{+2}$ ).

**9-(4-chlorophenyl)-3,4,6,7-tetrahydro-3,3,6,6-tetramethyl-10-phenylacridine-1,8(2H,5H,9H,10H)-dione (4b);**

<sup>1</sup> **H-NMR (CDCl<sub>3</sub>, 300 MHz):** δ = 7.24–7.28 (m, 4H), 7.48 (m, 3H), 7.3 (d, 2H), 5.20 (s, 1H), 2.12 (d, 2H), 2.21 (d, 2H), 1.83 (d, 2H), 1.09, (d, 2H), 1.01 (s, 6H, 2X CH<sub>3</sub>), 0.82 (s, 6H, 2X CH<sub>3</sub>); **IR (KBr):** 2960 cm<sup>-1</sup> (C-H stretch), 1595 cm<sup>-1</sup> (C = O), 1495 cm<sup>-1</sup> (C = C), 1360 cm<sup>-1</sup> (C-N).

## 4. Catalyst Characterizations

### 4.1 XRD Analysis:

The powder X-ray diffraction pattern of pure SiO<sub>2</sub> and In<sub>2</sub>O<sub>3</sub> is shown in Fig. 2(a) and 2(b) respectively. The pure SiO<sub>2</sub> sample consists of a broad diffraction pattern because it is amorphous in nature. The pure In<sub>2</sub>O<sub>3</sub> sample exhibit highly intense and sharp peak due to it is crystalline in nature. The X-ray diffraction patterns of a series of In<sub>2</sub>O<sub>3</sub>-SiO<sub>2</sub> catalysts calcined at 500°C in the presence of air for 2 h are shown in Fig. 2(c, d, e). As per results from X-ray powder diffractions, pure metal oxides and mixed metal oxides samples differ very much indicating incorporation of In<sub>2</sub>O<sub>3</sub> into SiO<sub>2</sub> to form In<sub>2</sub>O<sub>3</sub>-SiO<sub>2</sub> mixed metal oxides.

The study of XRD patterns shows, an interesting observation that the pure SiO<sub>2</sub> sample exhibits a diffraction pattern due to the formation of hexagonal solid, the broad peaks were obtained at 2θ = 21.74° corresponding to the planes (100) indicates the hexagonal structure of SiO<sub>2</sub>. The In<sub>2</sub>O<sub>3</sub> X-ray diffraction pattern having highly intense peaks are observed at 2θ = 21.56°, 30.67°, 35.55°, 51.12° and 60.77° corresponding to the planes (211), (222), (400), (440) and (622) indicate the cubic structure of In<sub>2</sub>O<sub>3</sub>. While the monoclinic phase could be identified match with JCPDS card no 76-0152 in case of a series of In<sub>2</sub>O<sub>3</sub>-SiO<sub>2</sub>, the XRD pattern data displayed in Fig. 2(c, d, e). In each case highly intense and sharp peaks were obtained at 2θ = 21.51°, 30.58°, 35.46°, 37.66°, 41.85° corresponding to the planes (-101), (-211), (120), (-231), (-320) respectively. It has been seen that, X-ray powder diffraction patterns of a series of In<sub>2</sub>O<sub>3</sub>-SiO<sub>2</sub> samples are crystalline in nature, indicating a strong interaction between the In<sub>2</sub>O<sub>3</sub> and SiO<sub>2</sub> support.

#### ESTIMATION OF PARTICLE SIZE USING DEBYE-SCHERRER EQUATION

The average crystallite size (T) of different ratio In<sub>2</sub>O<sub>3</sub>-SiO<sub>2</sub> solid materials can be estimated from X-ray line broadening using the Debye-Scherrer equation.

$$T = \frac{0.94\lambda}{\beta \cos\theta}$$

Where, T = average particle size, λ = wavelength, θ = diffraction angles, β = FWHM (Full width half maximum). The average crystallite sizes of SiO<sub>2</sub>, In<sub>2</sub>O<sub>3</sub> and different ratio In<sub>2</sub>O<sub>3</sub>-SiO<sub>2</sub> materials are

summarized in Table 6.

Table 6  
The average particle size estimation of prepared metal oxide and mixed metal oxide calcined at 500<sup>o</sup> C.

Entry	Metal Oxides	Ratio	Crystallite Size (nm)
1	SiO <sub>2</sub>	1	11
2	In <sub>2</sub> O <sub>3</sub>	1	30
3	In <sub>2</sub> O <sub>3</sub> -SiO <sub>2</sub>	0.8 : 0.2	36
4	In <sub>2</sub> O <sub>3</sub> -SiO <sub>2</sub>	0.2 : 0.8	40
5	In <sub>2</sub> O <sub>3</sub> -SiO <sub>2</sub>	1:1	23

## 4.2 FTIR ANALYSIS:

**Fig.3(a)** shows the FT-IR spectrum of the synthesized SiO<sub>2</sub> material. The absorption band at 3400 cm<sup>-1</sup> is due to the Si-OH stretching vibration, 2337 cm<sup>-1</sup> for glass SiO<sub>2</sub>, 1527 cm<sup>-1</sup> for the Si-OH bending mode, 1095 cm<sup>-1</sup> for Si-O stretching vibration and 802 cm<sup>-1</sup> due to the Si-O-Si bending vibration mode.

**Fig.3(b)** shows the FT-IR spectrum of In<sub>2</sub>O<sub>3</sub> metal oxide having an absorption band at 3390 cm<sup>-1</sup> which is due to the In-OH stretching vibration. The strong absorption band at 493 cm<sup>-1</sup> is due to the antisymmetric In-O-In vibrational mode of In<sub>2</sub>O<sub>3</sub> metal oxide. **Fig.3(c)** shows the FT-IR spectra of the In<sub>2</sub>O<sub>3</sub>-SiO<sub>2</sub> materials having absorption band at 3410 cm<sup>-1</sup> due to the Si-OH stretching vibration, 1689 cm<sup>-1</sup> due to the Si-OH bending mode, 1087 cm<sup>-1</sup> for Si-O stretching vibration and 810 cm<sup>-1</sup> due to the Si-O-Si bending vibrational mode the strong absorption band at 462 cm<sup>-1</sup> is due to the antisymmetric In-O-In vibrational mode of In<sub>2</sub>O<sub>3</sub> [47-49].

From the above FTIR data of metal oxide In<sub>2</sub>O<sub>3</sub>, SiO<sub>2</sub> and mixed metal oxide In<sub>2</sub>O<sub>3</sub>-SiO<sub>2</sub> are used to predict the plausibility structure by referencing their IR frequency. The oxidation state of the metals in the prepared In<sub>2</sub>O<sub>3</sub>-SiO<sub>2</sub> catalyst is In (III) and Si (IV).

## 4.3 SEM-EDS ANALYSIS:

The SEM produces artificial 3-dimensional point by point reconstruction of the sample from a signal emitted when the electron beam interacts with the specimen. When the beam interacts with the sample, several sorts of signals are produced two basic signals are electron and electromagnetic radiation. If SEM is operated so as to produce an image using backscattered electrons, it should be noted that resolution is considerably reduced in the back scattered mode of operation, because back scattered electrons are

generated in a large volume of sample (1–3 nm deep). In this study, it is necessary to consider not only intrinsic instrument resolution, but also the interaction of the incident electron beam and the sample. SEM and EDS measurements were applied to analyze the detailed morphology, surface roughness and structure of the material alongside element detection [50].

Figure 4(a) shows the flakes like structure of SiO<sub>2</sub> and Fig. 4(b) indicate the surface morphology of In<sub>2</sub>O<sub>3</sub> oxide shows grain like structure. Figure 4(c) indicates clearly deposition of In<sub>2</sub>O<sub>3</sub> on the surface of the SiO<sub>2</sub> metal oxide.

Elemental compositions of In<sub>2</sub>O<sub>3</sub>-SiO<sub>2</sub> metal oxide (Fig. 5), were represented in the EDS spectrum. The In, Si and O peaks can be obviously found in spectrum indicate that the In<sub>2</sub>O<sub>3</sub>-SiO<sub>2</sub> binary metal oxide particles were successfully prepared and there was complete removal of capping agent. The mass % of In, Si, O was found 2.75, 46.74, 50.51 shown in Table 7 and confirmed the presence of In, Si and O with corresponding empirical formula is **In<sub>1</sub> Si<sub>17</sub> O<sub>18</sub>**.

Table 7  
EDS elemental quantitative analysis of  
In<sub>2</sub>O<sub>3</sub>-SiO<sub>2</sub> (1:1).

Constituents	Mass (%)	Atom (%)
In	12.97	2.75
Si	53.87	46.74
O	33.17	50.51
Total	100.00	100.00

## 4.4 TEMPERATURE PROGRAMMED DESORPTION (NH<sub>3</sub>-TPD)

Temperature programmed desorption (NH<sub>3</sub>-TPD) measurements were carried out by analytical instrument MICROMERITICS CHEMISORB 2750 TPD/TPR. Temperature programmed desorption (TPD) studies were done using 100 mg of the sample loaded on a quartz reactor. The samples were first treated with 150°C in helium flow 25cc/min for 1 hour at room temperature. Desorption was carried out at a heating rate of 10°C/ min. Temperature programmed desorption of ammonia serves as a dependable technique for the quantitative determination of the acid strength distribution. After cooling to room temperature, ammonia was injected in the absence of the carrier gas flow and the system was allowed to attain equilibrium. A current of nitrogen was used to flush out the excess and physisorbed ammonia. The temperature was then raised in a stepwise manner at a linear heating rate of about 10°C/ min. The ammonia desorbed from 100°C to 500°C.

Temperature programmed desorption method (NH<sub>3</sub>-TPD) was used to determine the acidic properties of solid catalyst. This provides information about the total concentration and strength of acidic sites (Bronsted and Lewis). From TPD analysis data, it was found that the ammonia desorbed in region volume of 0.7236 mmol/gm of NH<sub>3</sub> desorbed at 190.38°C, it indicates that In<sub>2</sub>O<sub>3</sub>-SiO<sub>2</sub> (1:1) possesses weak acidic sites 0.02957 mmol/gm (Fig. 6).

## 4.5 BET ANALYSIS:

BET surface area was measured by means of N<sub>2</sub> adsorption at 77.74 K performed on a Micromeritics, ASAP 2010. BET theory aims to explain the physical adsorption of gas molecules on a solid surface and proved as an important analysis technique for the measurement of the specific surface area of a material is the so-called BET method (Brunauer, Emmett and Teller). N<sub>2</sub> adsorption-desorption isotherms provide information on the textural properties of In<sub>2</sub>O<sub>3</sub>-SiO<sub>2</sub> (1:1) and the specific surface area. The specific surface area and average pore diameter of In<sub>2</sub>O<sub>3</sub>-SiO<sub>2</sub> (1:1) are to be found 62.6013 m<sup>2</sup>/g and 8.82 nm Fig. 7 and Fig. 8.

## Conclusion

In summary, Due to the combination of In and Si metals to form the efficient and cost effective catalyst has been developed for the synthesis of acridine derivatives. We take the help of XRD, SEM, TEM, EDS, BET and FTIR characterization techniques for the analysis of surface morphology, shape, elemental composition, particle size and structure respectively of In<sub>2</sub>O<sub>3</sub>-SiO<sub>2</sub> catalytic material. We have developed a straight forward and efficient methodology for synthesis 1, 8 dioxo-decahydro acridine derivatives by using dimedone, substituted benzaldehyde and aniline under reflux condition using In<sub>2</sub>O<sub>3</sub>-SiO<sub>2</sub> catalyst in ethanol as solvent. The In<sub>2</sub>O<sub>3</sub>-SiO<sub>2</sub> catalyst is high thermal stability and reusability without any noticeable loss of reactivity. The mild reaction conditions, high catalytic activity and simplicity of the procedure offers several advantages such as non-toxic, non-corrosive, shorter reaction time, simple experimental procedure, high yield and catalyst can be recycled and reused.

## Declarations

### Acknowledgment

We are grateful to the Head, Department of Chemistry, Dr. B.A.M. University, Aurangabad-431004 (MS), India for providing the laboratory facility, and to the STIC Cochin, SAIF Chandigarh and IIT Bombay for characterization facilities. Author also thankful to the Principal, Mahant Jamnadas Maharaj Arts, Commerce and Science College, Karanjali.

### Competing interests

There are no conflicts of interest/competing interests to declare.

# References

1. R. M. Acheson, *Acridines*, 2<sup>nd</sup> edn. (John Wiley & Sons, 1972), pp. 1-14

---

2. C. Browning, J. Cohen, R. Gaunt, R. Gulbransen, *Proceeding of Royal soc.* **93**, 329 (1922)

---

3. R. Kumar, M. Kaur, M. Kumar, *Acta. Poloniae. Pharma. Drug Res.* **69**, 3 (2012)

---

4. A. Plodek, F. Bracher, *Mar. Drugs.* **14**, 26 (2016)

---

5. A. Fernandez, C. Valdes, *Open Me. Chem. J.* **5**, 11 (2011)

---

6. P. Zade, M. Ramana, *A.I.J.R.F.A.N.S.* **7**, 74 (2014)

---

7. O. Fadhel, R. Pretsch, *European Patent* 2312663, 1 (2011)

---

8. H. Soliman, T. Salama, *O.C.A.I.J.* **10**, 63 (2014)

---

9. H. Alinezhad, S. M. Tavakkoli, *Sci. World J.* 1 (2013)

---

10. A. Amani, S. Gholamzadeh, M. Zarenezhad, A. Malekpour, E. Javidnezhad, *J. Adv. Med. Sci. Appl. Technol.* **1**, 78 (2015)

---

11. R. Ferreira, A. Avino, S. Mazzini, R. Eritja, *Molecules.* **17**, 7067 (2012)

---

12. G. Cholewinski, K. Dzierzbicka, A. Kotdziejczyk, *Pharm. Reports.* **63**, 305 (2011)

---

13. J. Cookson, R. Heald, M. Stevens, *J. Med. Chem.* **48**, 7198 (2005)

---

14. M. Preobrazhenskaya, A. Shchekotikhin, A. Shtil, H. Huang, *J. Med. Sci.* **26**, 1 (2006)

---

15. J. Stanslas, D. Hagan, M. Ellis, C. Turner, J. Carmichael, W. Ward, T. Hammonds, M. Stevens, *J. Med. Chem.* **43**, 1563 (2000)

---

16. P. Kumar, R. Kumar, D. Prasad, *Arabian J. Chem.* **6**, 79 (2013)

---

17. G. Ziaran, A. Badiei, M. Hassanzadeh, S. Mousavi, *Arabian J. Chem.* **7**, 335 (2014)

---

18. M. Wainwright, *J. Antimicro. chemotherapy.* **47**, 1 (2001)

---

19. C. Ornelas, *New J. Chem.* **35**, 1973 (2011)

---

20. E. Olasik, P. Szymanski, E. Zurek, *Indian J. Experi. Bio.* **45**, 315 (2007)

- 
21. B. Philippe, B. Johann, G. Thomas, T. Martin, *Curr. Medicinal Chem. Anticancer agent.* **7**, 139 (2007)
- 
22. P. Francis, A. Palmer, M. Snape, G. Wilcock, *J. Neurol. Neurosurg. Psychiatry.* **66**, 137 (1999)
- 
23. B. Maleki, R. Tayebee, M. Kermanian, S. Ashrafi, *J. Mex. Chem. Soc.* **57**, 290 (2013)
- 
24. G. Ziarani, A. Badiei, M. Hassanzadeh, S. Mousavi, **7**, 335 (2014)
- 
25. F. Hatamjafari, O. Lazarjani, *Rev. Roum. Chim.* **62**, 255 (2017)
- 
26. A. Dorehgirae, E. Kermani, H. Khabazzadeh, *J. Chem. Sci.* **126**, 1039 (2014)
- 
27. M. Kiani, M. Mohammadipour, *RSC Adv.* **7**, 997 (2017)
- 
28. N. Biswas, D. Srimani, *J. Org. Chem.* **86**, 9733 (2021)
- 
29. S. Vahdat, M. Akbari, *J. Chem.* **27**, 1573 (2011)
- 
30. D. Tayde, A. Yelwande, B. Arbad, M. Lande, *Indian Chem. Soc.* **91**, 807 (2014)
- 
31. D. Tayde, M. Lande, *Chem. Rev. Lett.* **4**, 30 (2021)
- 
32. D. Tayde, A. Yelwande, M. Navgire, M. Lande, *Chem. Sci. Rev. Lett.* **4**, 252 (2015)
- 
33. M. Navgire, A. Yelwande, D. Tayde, B. Arbad, M. Lande, *Chinese J. Catal.* **32**, 261 (2012)
- 
34. M. Chen, J. Wu, Y. Liu, Y. Cao, L. Guo, H. He, K. Fan, *Appli. Cataly. A: General.* **407** 20 (2011)
- 
35. K. Fatema, S. Sagadevan, Y. Liu, K. Cho, C. Jung, W. Oh, *J. Materials Sci.* **55**, 13085 (2020)
- 
36. P. Dyson, P. Jessop, *Catal. Sci. Technol.* **6**, 3302 (2016)
- 
37. J. Broos, M. Martin, I. Rouwenhorst, W. Verboom, D. Reinhoudt, *Recl. Trav. Chim. Pays-Bas.* **110**, 222 (1991)
- 
38. C. Balny, A. Hooper, *Eur. J. Biochem.* **176**, 273 (1998)
- 
39. I. McManus, H. Daly, J. Thompson, E. Connor, C. Hardacre, S. Wilkinson, N. Bonab, J. Damc, M. Simmons, E. Stitt, C. Agostino, J. McGregor, L. Gladden, J. Delgado, *J. Catal.* **330**, 344 (2015)
-

40. M. Kanatzidis, K. Poeppelmeier, *Prog. Solid State Chem.* **36**, 1 (2007)

---

41. D. Segal, *J. Mater. Chem.* **7**, 1297 (1997)

---

42. M. Potdar, G. Kelso, L. Schwarz, C. Zhang, M. Hearn, *Molecules.* **20**, 16788 (2015)

---

43. H. Luo, Y. Kang, H. Nie, L. Yang, *J. Chin. Chem. Soc.* **55**, 1280 (2008)

---

44. D. Q. Shi, J. W. Shi, H. Yao, *Synth. Commun.* **39**, 664 (2009)

---

45. B. Das, P. Thirupathi, I. Mahender, V. Saidi Reddy, Y. K. Rao, *J. Molecular Catal. A: Chem.* **247**, 233 (2006)

---

46. Z. Q. Tang, Y. Chen, C. N. Liu, K. Y. Cai, S. J. Tu, *J. Heterocycl. Chem.* **47**, 363 (2010)

---

47. R. Nariyal, P. Kothariand, B. Bisht, *Chem. Sci. Trans.* **3**, 1064 (2014)

---

48. S. Bhardwaj, N. Bhardwaj, M. Kukkar, A. Sharma, K. Kim, A. Deep, *Sensors.* **15**, 31930 (2015)

---

49. G. Liu, *Int. J. Electrochem. Sci.* **6**, 2162 (2011)

---

50. A. Gira, G. Caputo, M. Ferro, *Comprehensive Ana. Chem.* **75**, 153 (2017)

## Note

See the Supplemental Files section for schemes and other images and structures found in the paper.

## Figures

The recyclability of  $\text{In}_2\text{O}_3\text{-SiO}_2$  for synthesis of 1,8dioxo-decahydroacridine .

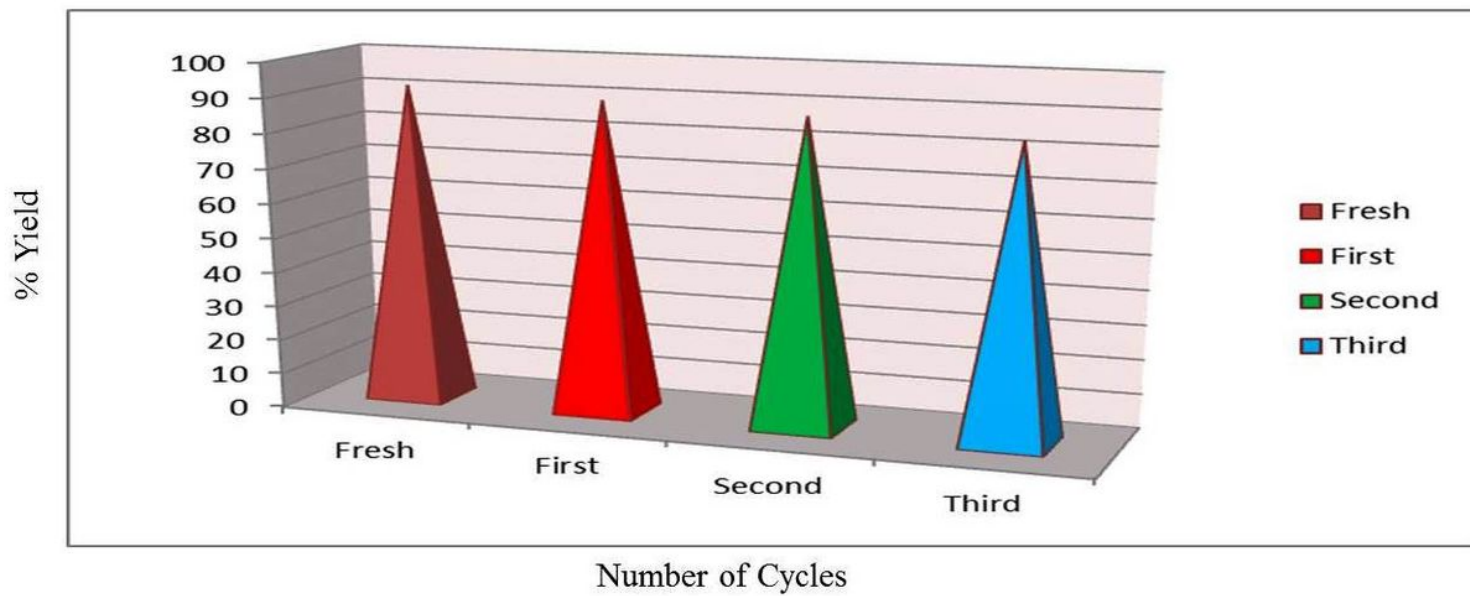


**Figure 1**

The recyclability of  $\text{In}_2\text{O}_3\text{-SiO}_2$  (1:1) for synthesis of 1,8-dioxo-decahydroacridine. Proposed mechanism pathway of 1,8-dioxo-decahydroacridine derivatives.

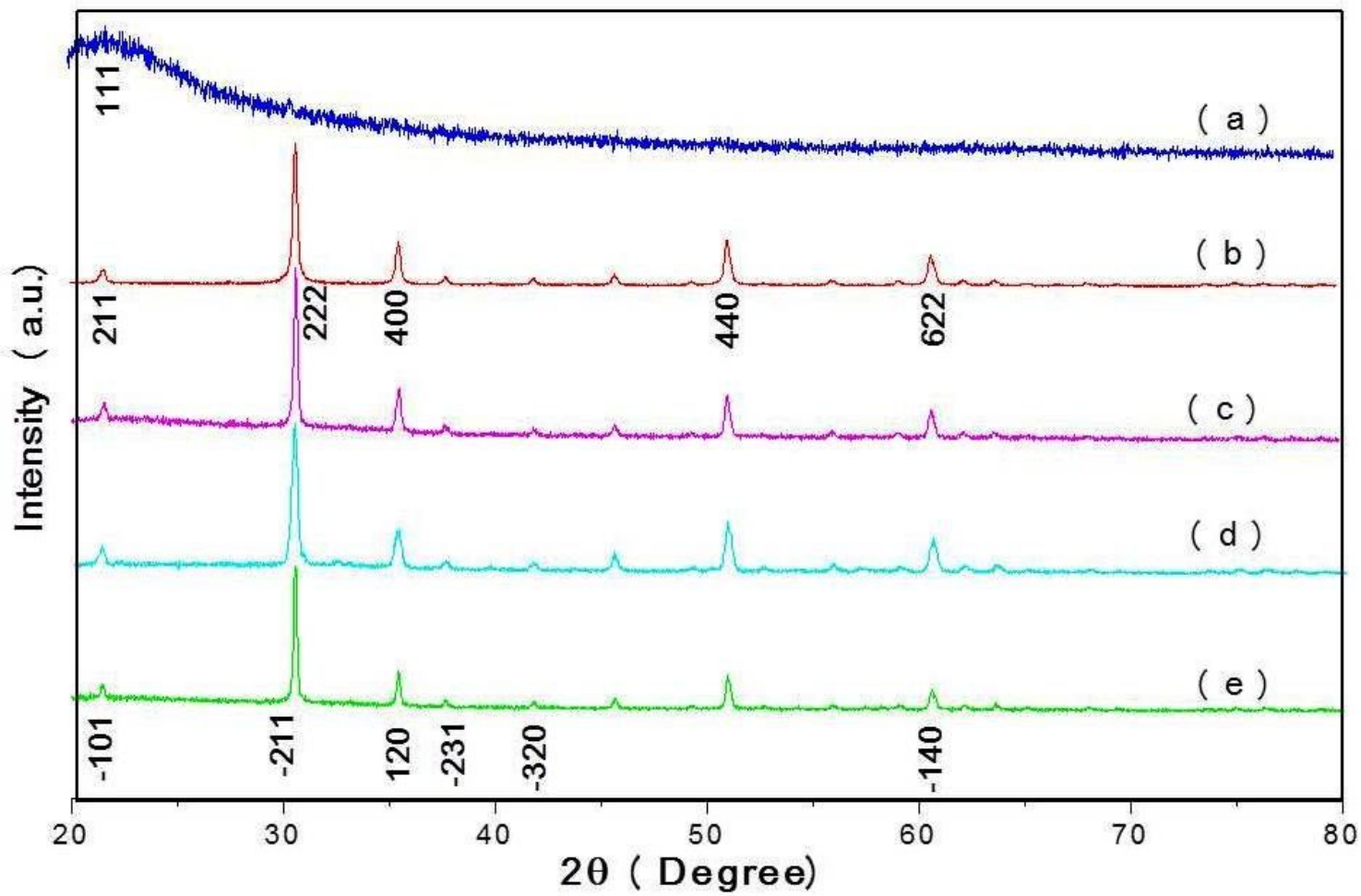


Figure 2

XRD patterns of (a) SiO<sub>2</sub> (b) In<sub>2</sub>O<sub>3</sub> and (c) In<sub>2</sub>O<sub>3</sub>-SiO<sub>2</sub> (0.8-0.2) (d) In<sub>2</sub>O<sub>3</sub>-SiO<sub>2</sub> (0.2-0.8) (e) In<sub>2</sub>O<sub>3</sub>-SiO<sub>2</sub> (1-1).

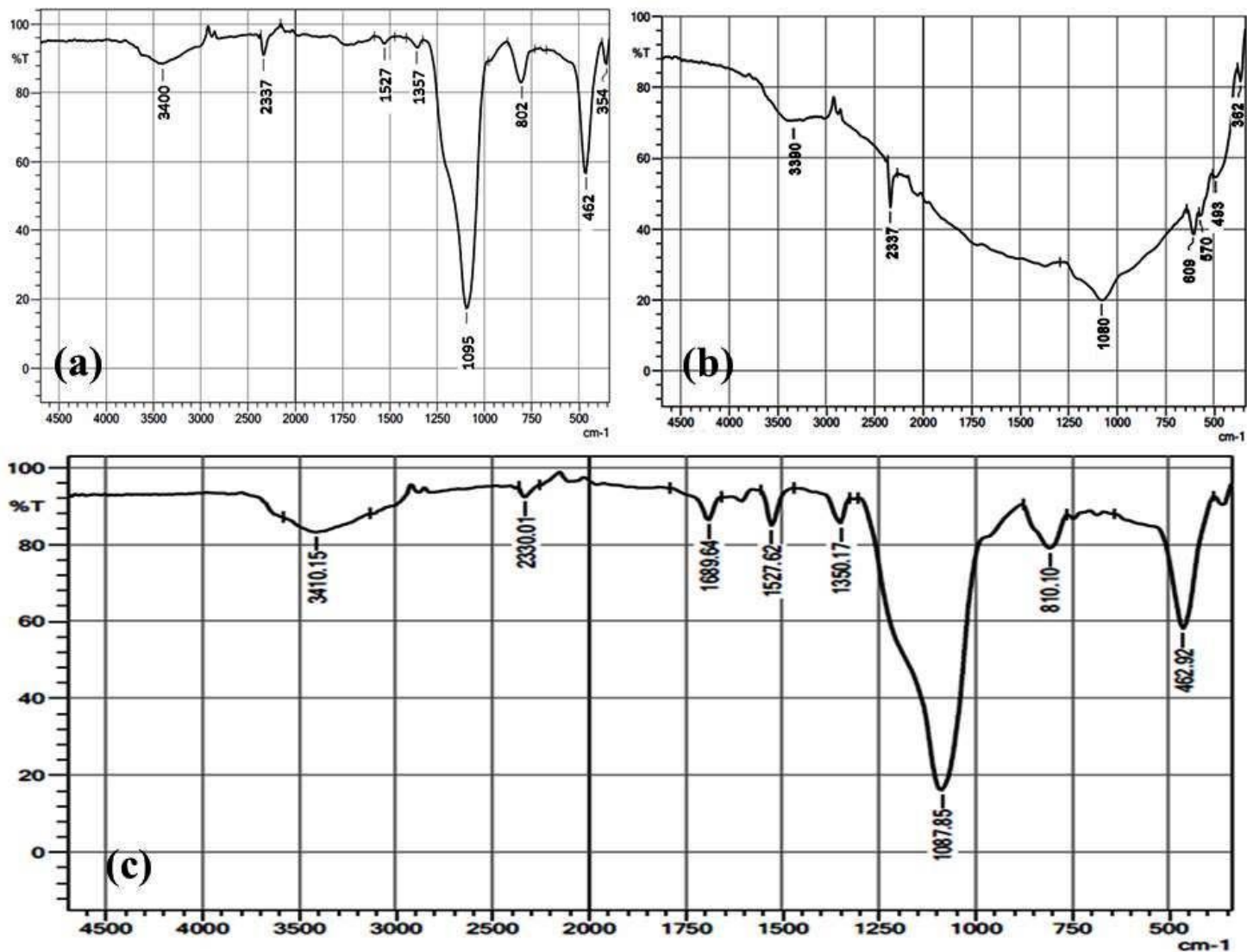


Figure 3

FTIR spectrum of a) SiO<sub>2</sub>, b) In<sub>2</sub>O<sub>3</sub>, and c) In<sub>2</sub>O<sub>3</sub>-SiO<sub>2</sub> (1:1).

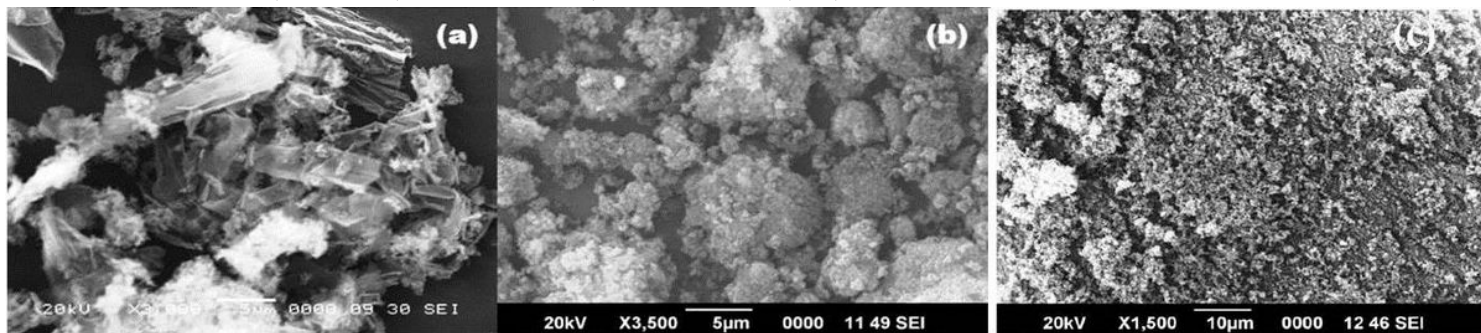
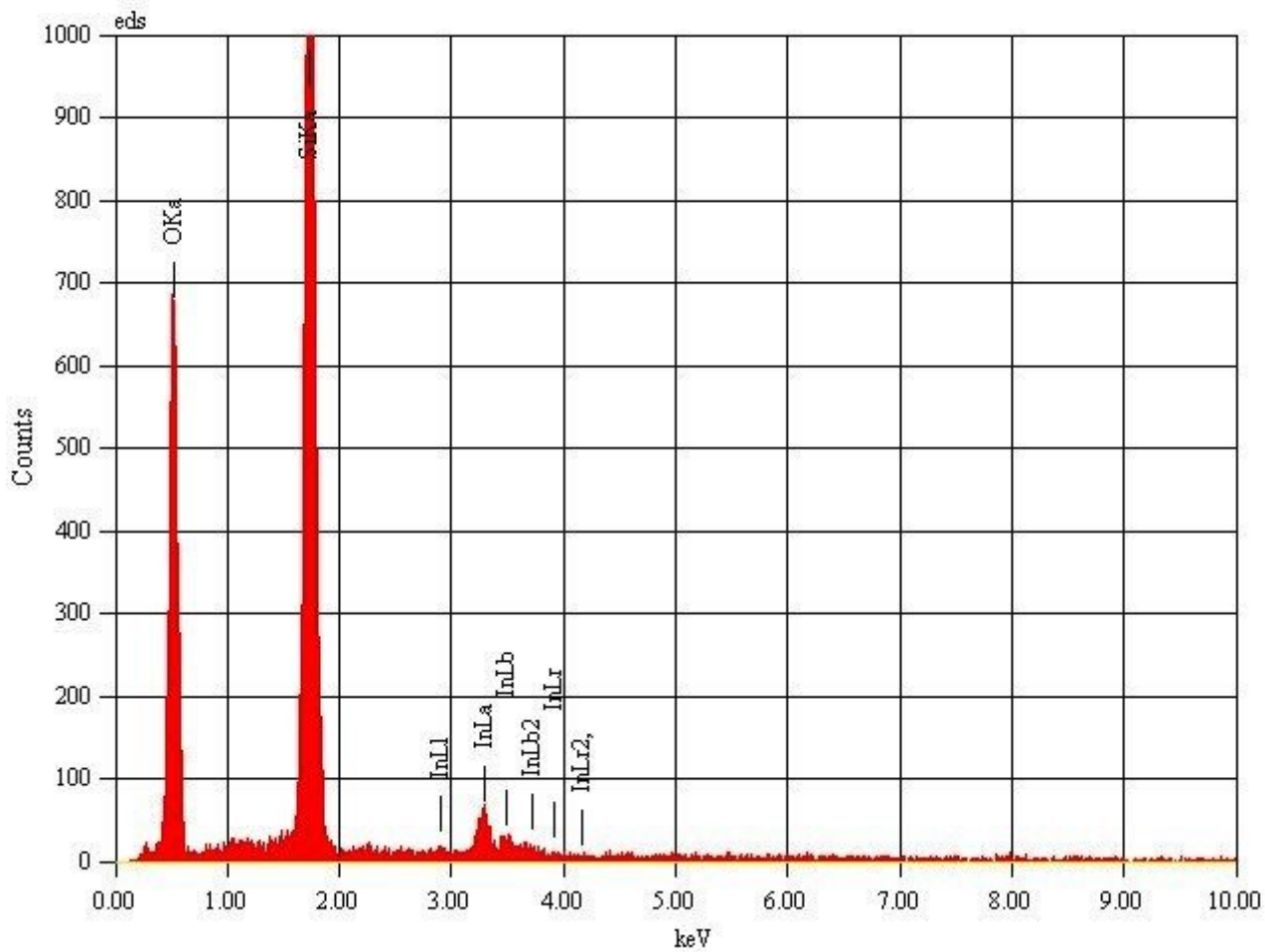


Figure 4

SEM image of a) SiO<sub>2</sub> and b) In<sub>2</sub>O<sub>3</sub> (c) In<sub>2</sub>O<sub>3</sub>-SiO<sub>2</sub> (1:1)



**Figure 5**

EDS spectrum of In<sub>2</sub>O<sub>3</sub>-SiO<sub>2</sub> (1:1).

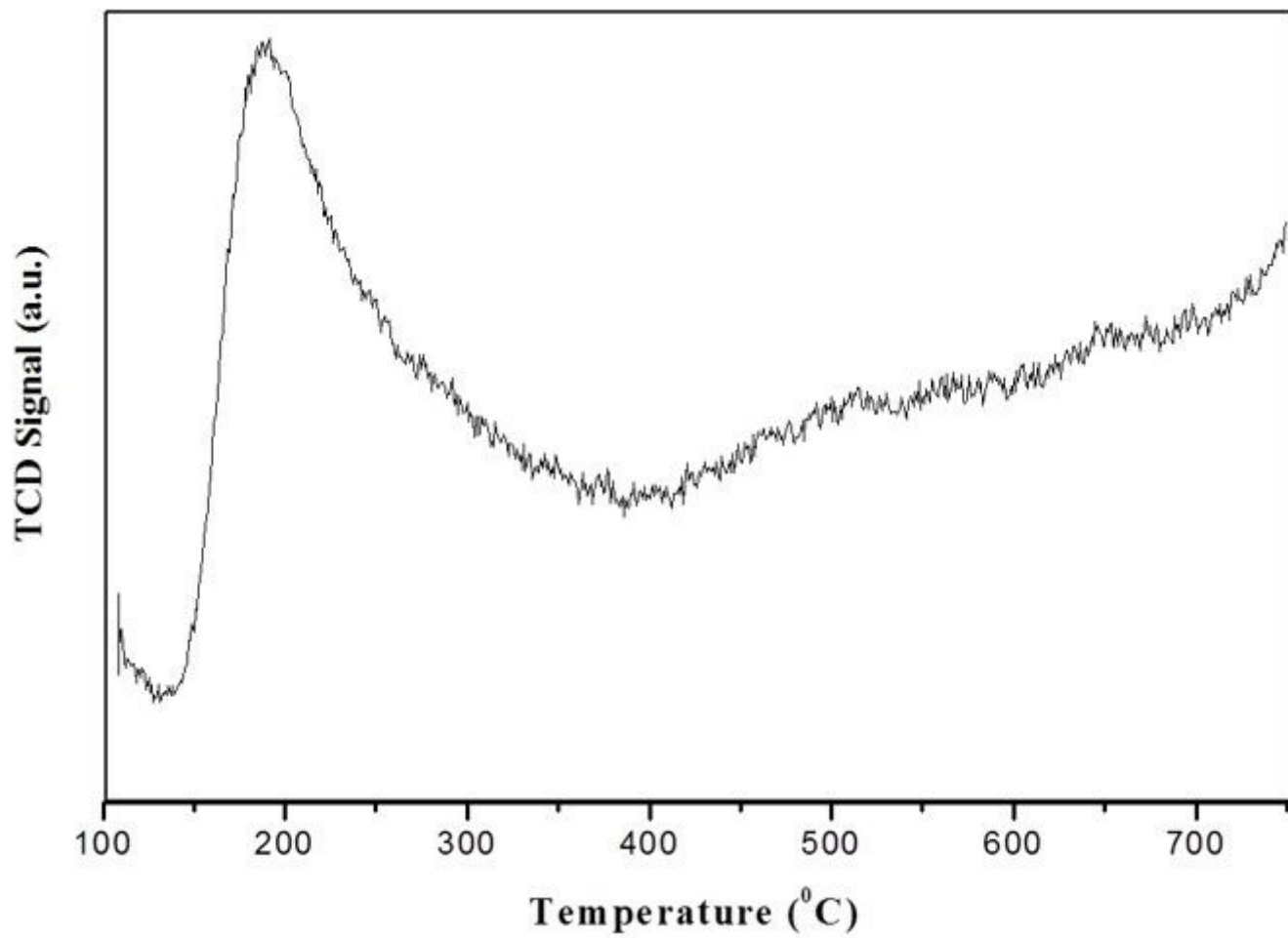


Figure 6

NH<sub>3</sub>-TPD profiles of In<sub>2</sub>O<sub>3</sub>-SiO<sub>2</sub> (1:1).

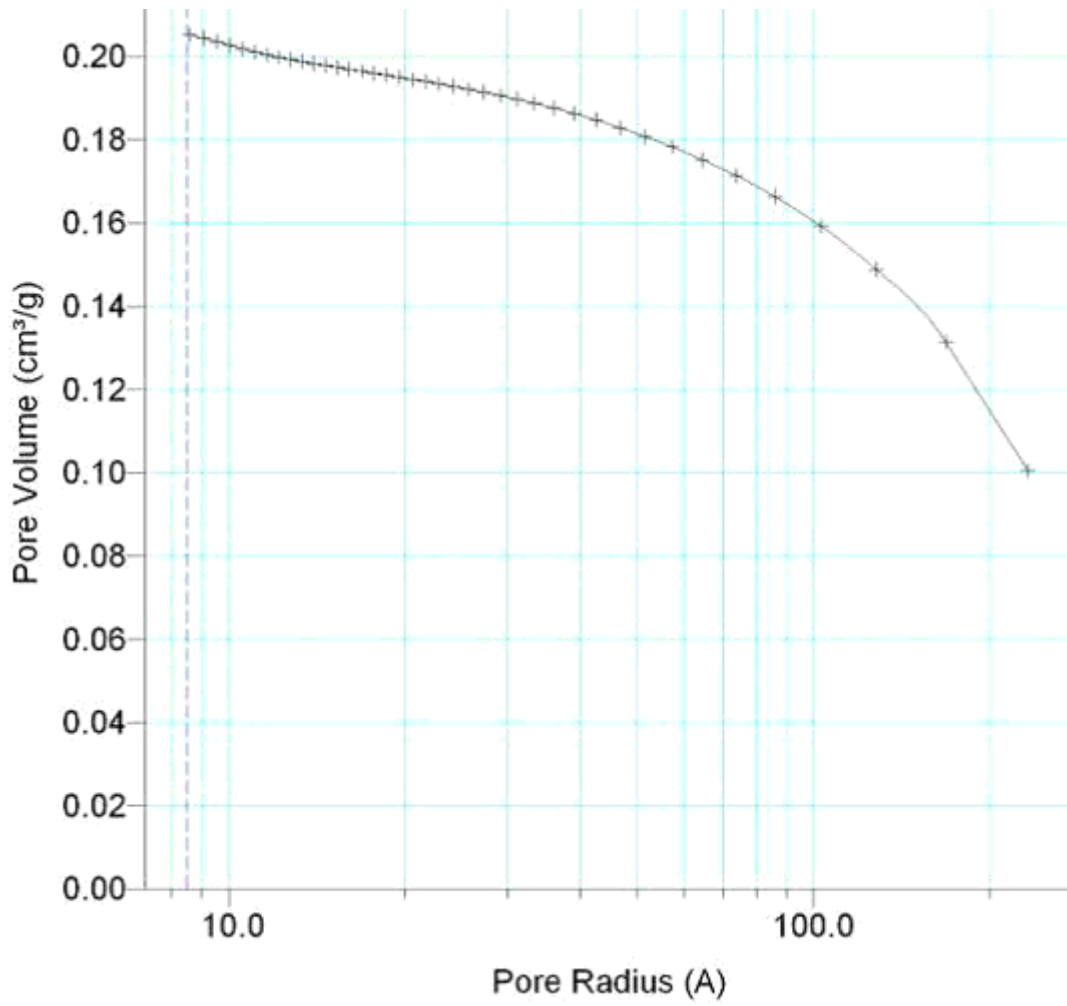
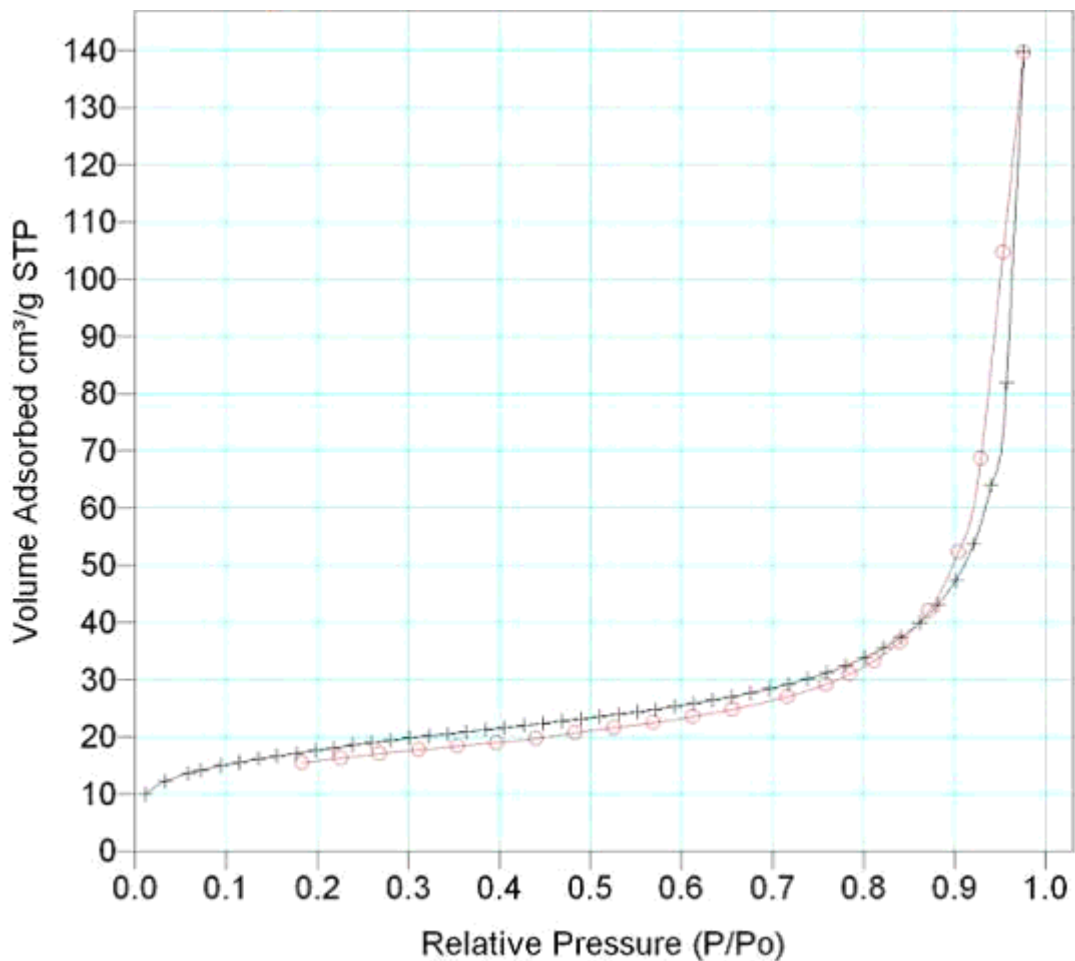


Figure 7

N<sub>2</sub> adsorption/desorption isotherm of In<sub>2</sub>O<sub>3</sub>-SiO<sub>2</sub> (1:1).



**Figure 8**

BJH adsorption Cumulative pore diameter In<sub>2</sub>O<sub>3</sub>-SiO<sub>2</sub> (1:1).

## Supplementary Files

This is a list of supplementary files associated with this preprint. Click to download.

- [GraphicalAbstract.png](#)
- [Image.png](#)
- [Scheme1.jpg](#)
- [Image.png](#)